

## Abnormal Bone Mineral Maturation in the Chronic Uremic State

Jean E. Russell, ... , John D. Termine, Louis V. Avioli

*J Clin Invest.* 1973;52(11):2848-2852. <https://doi.org/10.1172/JCI107480>.

**Research Article**

X-ray diffraction analysis of bone from chronically uremic but nonacidotic rats with normocalcemia and hyperphosphatemia revealed smaller apatite crystals and an increase in the X-ray amorphous mineral fraction when compared to age-matched, pair-fed control animals, indicating less advanced mineral maturation in the uremic animals. Studies in animals with varied degrees of chronic renal insufficiency revealed a progression of the bone crystal maturational defect with advancing uremia.

**Find the latest version:**

<https://jci.me/107480/pdf>



# Abnormal Bone Mineral Maturation in the Chronic Uremic State

JEAN E. RUSSELL, JOHN D. TERMINE, and LOUIS V. AVIOLI

*From the Department of Medicine, Jewish Hospital of St. Louis and Washington University School of Medicine, St. Louis, Missouri 63110 and the Molecular Structure Section, Laboratory of Biological Structure, National Institute of Dental Research, National Institutes of Health, Bethesda, Maryland 20014*

**ABSTRACT** X-ray diffraction analysis of bone from chronically uremic but nonacidotic rats with normocalcemia and hyperphosphatemia revealed smaller apatite crystals and an increase in the X-ray amorphous mineral fraction when compared to age-matched, pair-fed control animals, indicating less advanced mineral maturation in the uremic animals. Studies in animals with varied degrees of chronic renal insufficiency revealed a progression of the bone crystal maturational defect with advancing uremia.

## INTRODUCTION

Although a causal relationship between chronic renal failure and progressive osteopenia has been well documented by radiographic and histochemical analyses (1, 2), the sequence of physiology and biochemical events that initiate and perpetuate the derangements in skeletal metabolism are still poorly defined. Previous investigations have been concerned primarily with rates of bone mineral (apatite) and matrix (collagen) turnover, under the assumption that the intricate processes of crystal growth and collagen maturation were proceeding in normal fashion. In an earlier study, we demonstrated maturational alterations in bone collagen and mineral metabolism in the experimental uremic state that progressed with advancing uremia, although insignificant alterations in plasma pH, calcium, and bone carbonate content obtained (3). The present study was undertaken to determine whether the apparent collagen maturational defect in the advancing uremic state is associated with compositional and structural alterations of the mineral components of skeletal tissue.

Dr. Russell is the recipient of NIH postdoctoral research grant AM-50025.

Received for publication 7 March 1973 and in revised form 25 June 1973.

## METHODS

Female Holtzman rats at 6 wk of age were unilaterally nephrectomized with contralateral segmental renal infarction, resulting in an impairment of 7/8 normal kidney function as previously described (3). This ischemic infarction of functioning renal mass persisted during the subsequent 2, 5, or 9-wk period of study. Control animals were pair-fed to maintain similar rates of growth between the two experimental groups. At the time of sacrifice all animals were exsanguinated and the tibia immediately excised, cleaned of excess soft tissue, and frozen in dry ice. Bones from groups of pair-fed control and uremic rats were analyzed at 2, 5, and 9-wk stages of renal insufficiency. As reported in earlier studies, the uremic state was attended by elevation in plasma, inorganic phosphate (controls,  $7.76 \pm 0.18$ , uremics  $9.66 \pm 0.33$  mg/100 ml); creatinine (controls  $0.56 \pm 0.02$ , uremics  $1.24 \pm 0.05$  mg/100 ml); and urea nitrogen (control,  $24.4 \pm 2.8$ , uremics  $56.0 \pm 2.6$  mg/100 ml). Plasma pH and calcium values in the uremic animals were  $7.41 \pm 0.04$  and  $10.24 \pm 0.10$  mg/100 ml, respectively, and comparable to those obtained in the control group ( $7.40 \pm 0.01$ , and  $10.23 \pm 0.34$  mg/100 ml, respectively). Calcium content of ashed skeletal samples was determined by atomic absorption spectrometry and phosphate by the method of Gee and Deitz (4). Carbonate content of deproteinated samples was determined by a modified micro-diffusion technique (5).

Analysis of bone mineral structure was performed via quantitative X-ray diffraction (XRD)<sup>1</sup> after removal of the epiphyseal plate and extraction of organic matter with 95% hydrazine at 55°C as reported elsewhere (5). The rationale and experimental protocol for these XRD measurements is as follows. Upon quantitation, it has been found that the total mineral contained in either lyophilized or hydrazine-deproteinated bone specimens exhibits markedly less integrated XRD intensity than fully crystalline synthetic apatites (5-8). In order for such a comparison to be valid, however, both the bone mineral specimen and the synthetic apatite standard must have almost identical (a) total chemical compositions; (b) total XRD curve profiles (including quantitative degree of peak broadening in both the apatite  $\bar{a}$ - (width) and  $c$ - (length) crystal axes); and

<sup>1</sup> Abbreviations used in this paper: ACP, amorphous calcium phosphate; XRD, X-ray diffraction.

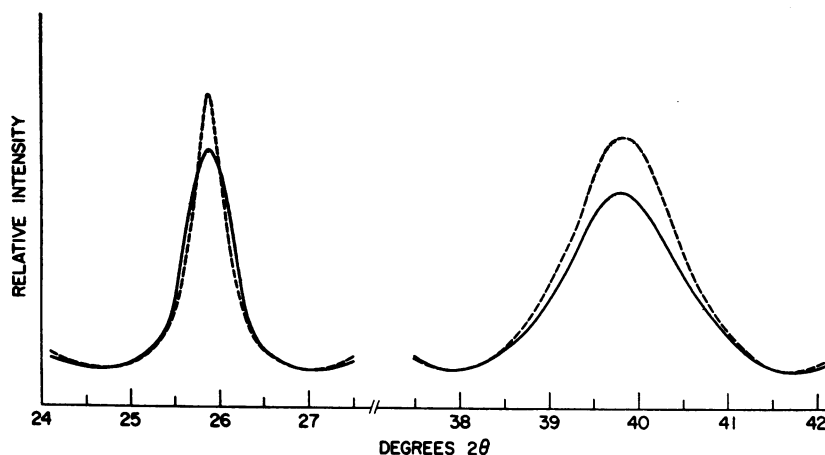


FIGURE 1 XRD patterns from control (dashed line curves) and 9-wk-uremic (solid line curves) rat bones in the apatite (002) [ $\bar{c}$ -axis] and (310) [ $\bar{a}$ -axis] reflections.

(c) predominant crystal ultrastructures (including average dimensions as well as shape) as determined in the electron microscope (5). If those criteria are satisfied, this difference in XRD intensity can be attributed to the presence of nondiffracting mineral components in the bone specimens under study (5-8). The degree that a given bone sample deviates in integrated XRD intensity from such a fully crystalline, synthetic apatite standard is a measure, therefore, of that fraction of its total mineral that is "amorphous" to XRD (i.e., the percentage of X-ray amorphous mineral present). Conversely, the degree that a given bone sample agrees in integrated XRD intensity with a suitable synthetic standard is a measure of that fraction of its mineral that is fully crystalline to XRD.

The fully crystalline, synthetic apatite standards used to assess the percentage of X-ray amorphous mineral present in the bone samples examined in this study were a series of  $\text{CO}_3^{2-}$ -containing apatites the preparation and properties of which have been described in detail elsewhere (5, 9). These synthetic crystals have been shown to be quite similar to rat bone apatite in chemical composition, diffraction peak broadening, and crystal ultrastructure and as such serve as appropriate standards for this quantitative XRD analysis in rat bone specimens (5). As also described earlier, integrated XRD intensity for most synthetic apatites decreases slightly with increased diffraction peak broadening (8). A plot of integrated, orientation-independent XRD intensity ( $\text{I} \times \ln$  values, defined below) vs. the sum of the integral breadths from the apatite (002) and (310) reflections (measures of peak broadening in the  $\bar{c}$ - and  $\bar{a}$ -crystal axes, also defined below) for these carbonate-containing synthetics formed a straight line covering the range of diffraction peak broadening found for most rat bone specimens and having a slope of  $-0.65 \text{ I} \times \ln$  per combined integral breadth units with a correlation coefficient of  $-0.949$ . This curve is in general agreement with previously published data from other systems (8). As described previously (8), this plot was used as a standard curve in this study to obtain interpolated, fully crystalline XRD intensity values when comparing bone and synthetic apatite specimens with a given combined integral breadth in the range studied. Once this standard XRD intensity value was obtained, then the calculation of the percentage of X-ray amorphous mineral in the bone specimen under

study was calculated as described above and elsewhere (5, 8).

In this study, both integrated XRD intensity and peak broadening were measured from the synthetic standards as well as from the hydrazine-deproteinated bone powders (obtained by gentle hand-grinding in acetone, 1-2 min) by procedures only slightly modified from those described elsewhere (5). XRD patterns were recorded at 30 kV, 22 mA with a Siemens scintillation counter diffractometer (Siemens Corp., Medical Industrial Div., Iselin, N. J.), equipped with a graphite curved crystal monochromator set for  $\text{C}_K\text{-K}\alpha$  radiation. Entrance and receiving slits were  $0.5^\circ$  and  $0.4 \text{ mm}$ , respectively. Apatite  $\bar{c}$ -axis (002) reflections were step-scanned between  $23.60$  and  $27.60^\circ 2\theta$ , while  $\bar{a}$ -axis (310) reflections were step-scanned between  $36.00$  and  $44.00^\circ 2\theta$ . A scan rate of  $0.05^\circ/\text{step}$  and a counting period of  $80 \text{ s}/\text{step}$  were used in both cases. The data were collected with the aid of a standard teletype unit on-line to an in-house computer. For both the  $\bar{a}$ - and  $\bar{c}$ -axis tracings, four repetitive scans (obtained with the aid of a specially-designed automated sweeping device driving the step-scanner) were time-averaged with the aid of the computer in each instance. This computer program (available on request) also provides the integrated diffraction intensity as well as the integral breadth ( $\beta^1$ , peak area/peak height) and the half-width ( $\beta^2$ , width at half maximum peak intensity) for each curve processed. The latter two peak-broadening parameters are inversely proportional to average apatite crystal size and/or perfection in the crystal dimension measured. The resulting  $\bar{a}$ - and  $\bar{c}$ -axis XRD-integrated intensity values were normalized against a brass standard and added together in order to obtain an orientation-independent, integrated XRD intensity ( $\text{I} \times \ln$  value) for each specimen examined (5, 6).  $\text{I} \times \ln$  values were reproducible to within 1.5%, while the peak-broadening parameters ( $\beta^1, \beta^2$ ) were found to be reproducible to within 1.0-1.25% of the values obtained. Sample XRD curves obtained by this procedure for control and uremic animals are shown in Fig. 1.

The amount of X-ray amorphous bone mineral present in any given tissue has been found to decrease systematically with increasing degree of tissue maturation in the growing rat, chick, and fetal calf (7, 8, 10, 11). Simultaneously, that portion of the bone mineral that is fully

crystalline as measured by XRD increases in average crystallite size and/or perfection (as evidenced by decreased diffraction peak broadening) with increased tissue maturation (7, 8). Thus, "immature" bone tissue is characterized by both increased amounts of X-ray amorphous mineral and less perfect, smaller-sized, but XRD-detectable, apatite crystallites.

At first, it was assumed that the X-ray amorphous bone mineral fraction consisted almost entirely of a biological analogue to synthetic amorphous calcium phosphate (ACP). Calcium phosphate formation in vitro proceeds by the initial deposition of an ACP precursor phase, which subsequently transforms into tiny crystals of apatite (12). These crystals then rapidly increase in size through normal solution ripening (12). The relationship between this sequence of chemical reactions and the sequence of changes in average bone mineral diffraction properties accompanying normal tissue maturation as described above is reasonably analogous. Furthermore, like synthetic ACP specimens, the X-ray amorphous bone mineral fraction completely recrystallizes upon prolonged in vitro exposure to aqueous solutions (5, 12). In agreement with these findings, recent studies have indicated that a large portion of the X-ray amorphous mineral fraction of rat bone has physicochemical properties quite similar to those of the synthetic ACPs (5). However, it was also realized that the total X-ray amorphous bone mineral fraction encompasses more than just an ACP-like component (5). It has always been recognized, for example, that calcium and phosphate either individually or compositely bound to matrix or cellular components could contribute to the total bone mineral fraction amorphous to XRD. It was recently found that the total X-ray amorphous mineral fraction also contains small, tightly packed particles poorly crystalline to electron diffraction but which, because of several experimental factors, are amorphous to XRD fraction (5). The exact origin or role of these particles is not understood at present, but they most probably represent a less advanced stage of mineral development than the more clearly defined, plate-

like crystals of rat bone (5). Thus, even though the X-ray amorphous bone mineral fraction encompasses several components, it still represents, in physicochemical terms, a less mature form of mineral than the predominant, platelike apatite crystals of bone that are measurable by quantitative XRD. This is in full agreement, then, with the studies described above (7, 8, 10, 11) indicating that less fully developed or "immature" bone contains increased amounts of X-ray amorphous mineral and less perfect, smaller-sized (as evidenced by increased peak broadening or  $\beta^{\dagger}, \beta^{\ddagger}$  values) apatite crystals as measured by quantitative XRD.

## RESULTS

As illustrated in Table I, the rate of mineral maturation in the pair-fed control animals of this study was normal throughout the 15 experimental weeks. When compared to the results of previous rat bone studies (8), the percentage X-ray amorphous mineral values exhibit an appropriate age-related decrease while the  $\beta$  values correspondingly diminish, indicating a diminution in the relative amount of X-ray amorphous or immature bone mineral and an increase in the size and/or perfection of the more fully mature (XRD-measurable) crystalline apatite components. In contrast, %C values (i.e., percent crystallinity or  $100\% - \%ACP$ ) of uremic animals increased only minimally from 2 to 5 wks of uremia ( $P < 0.05$ ) and then remained unchanged as the uremia progressed to 9 wk (Table I). Furthermore, no change in bone crystal size and/or perfusion ( $\beta$  value) was observed during the entire course of renal failure, despite the advancing age of the animal. Typical XRD patterns from normal and uremic bones are shown in Fig. 1.

TABLE I  
XRD Data for Hydrazine-Deproteinized Tibia Taken from Experimentally Induced-Uremic and Pair-Fed Control Rats

Weeks of age at sacrifice	Weeks in uremic state before sacrifice	No. of animals	Peak-broadening parameters*		Integrated diffraction intensity $\ddagger$	X-ray amorphous mineral %
			$\beta^{\ddagger}$ (002) ( $^{\circ}2\theta$ )	$\beta^{\dagger}$ (310) ( $^{\circ}2\theta$ )		
Control animals						
8	0	3	$0.503 \pm 0.006$ §	$1.50 \pm 0.03$ §	$2.143 \pm 0.099$ §	$41.0 \pm 2.6$ §
11	0	3	$0.482 \pm 0.008$	$1.43 \pm 0.01$	$2.957 \pm 0.194$	$29.4 \pm 3.0$
15	0	4	$0.463 \pm 0.010$	$1.39 \pm 0.02$	$3.285 \pm 0.029$	$23.8 \pm 0.4$
Experimental animals						
8	2	3	$0.517 \pm 0.012$	$1.51 \pm 0.02$	$2.393 \pm 0.019$	$41.3 \pm 1.6$
11	5	3	$0.517 \pm 0.006$	$1.48 \pm 0.02$	$2.531 \pm 0.078$	$37.0 \pm 2.2$
15	9	4	$0.530 \pm 0.010$	$1.51 \pm 0.01$	$2.426 \pm 0.130$	$38.7 \pm 3.2$

\* These parameters are inversely proportional to crystal size and/or perfection.

$\ddagger$   $\ln$  values.

§ Mean  $\pm$  SD.

## DISCUSSION

The accumulated XRD data indicate that bone mineral maturation in uremic animals is less advanced, i.e., uremic bone contains both smaller (XRD-detectible) apatite crystals and a larger X-ray amorphous mineral fraction than normal bone. Comparison of the XRD data between each pair-fed control and uremic group (Table I) reveals that a statistical decrease in mineral maturation was not obtained until the 5-wk period of renal insufficiency ( $P < 0.01$ ). After 9 wk of uremia, however, the retardation in bone mineral maturation was further accentuated ( $P < 0.001$ ) with the amount of mature crystalline bone in the 15-wk-old uremic animals comparable to that observed in the 8-wk-old control group (Table I). These collective observations thus indicate that the progressive uremic state imposes a block in the orderly bone mineral maturational process. The alterations in mineral structure and/or maturation were associated with hyperphosphatemia and not accompanied by significant changes in bone carbonate content or Ca/P ratio, nor with detectable changes in plasma pH and calcium values. The 15-wk-old, pair-fed control animals had  $\text{CO}_3^{2-}$  contents of  $6.6 \pm 0.8\%$ ,<sup>2</sup> while the 15-wk-old experimental animals (9 wks uremic) had  $\text{CO}_3^{2-}$  contents of  $6.2 \pm 0.6\%$ .<sup>2</sup> The structural changes, therefore, probably cannot be attributed to a systemic acidosis or lack of inorganic constituents essential to normal bone maturation, although it has been well demonstrated that the chronic acidotic uremic state in man is associated with low bone carbonate (13, 14).

In our previous communication, alterations in collagen maturation were documented as early as the 2-wk period of experimentally induced uremia (3). These changes occurred well in advance of the inorganic structural alterations described in the present study. Since it is thought that maturation and increased cross-linking of newly synthesized collagen precedes calcification in hard tissues (15, 16), the altered maturational sequence attending experimental chronic uremia suggests that normal cell processes are, at the very least, sequentially perturbed at the bone level. The relationship of these data to reports of altered vitamin D metabolism in uremia (17) and to others citing defective collagen cross-linking in the vitamin D-deficient state (18) are yet to be defined. It is interesting to note, however, that experimental rachitic states are also characterized by an increase in the X-ray amorphous bone mineral fraction (8). Reported increments in skeletal magnesium content with advancing renal disease (19) may also contribute to the altered maturational sequence of bone apatite observed in the uremic animals, since the magnesium ion re-

<sup>2</sup> Data reflect means  $\pm$  standard deviation from several determinations of different samples of pooled tissues.

portedly retards the information of mature apatite by stabilizing the precursor, relatively immature, ACP phase (20).

## ACKNOWLEDGMENTS

This work was supported in part by NIH Contract 70-2219 and NIH grant AM-11674.

## REFERENCES

1. Garner, A., and J. Ball. 1966. Quantitative observations on mineralised and unmineralised bone in chronic renal azotaemia and intestinal malabsorption syndrome. *J. Pathol. Bacteriol.* **91**: 545.
2. Meema, H. E., S. Rabinovich, S. Meema, G. J. Lloyd, and D. G. Oreopoulos. 1972. Improved radiological diagnosis of azotemic osteodystrophy. *Radiology.* **102**: 1.
3. Russell, J., and L. V. Avioli. 1972. Effect of experimental chronic renal insufficiency on bone mineral and collagen maturation. *J. Clin. Invest.* **51**: 3072.
4. Gee, A., and V. R. Deitz. 1953. Determination of phosphate by differential spectrophotometry. *Anal. Chem.* **25**: 1320.
5. Termine, J. D., E. D. Eanes, D. J. Greenfield, M. U. Nylen, and R. A. Harper. 1973. Hydrazine-deproteinated bone mineral: physical and chemical properties. *Calcif. Tissue Res.* **12**: 73.
6. Harper, R. A., and A. S. Posner. 1966. Measurement of noncrystalline calcium phosphate in bone mineral. *Proc. Soc. Exp. Biol. Med.* **122**: 137.
7. Quinaux, N., and L. J. Richell. 1967. X-ray diffraction and infrared analysis of bone specific gravity fractions in the growing rat. *Isr. J. Med. Sci.* **3**: 677.
8. Termine, J. D., and A. S. Posner. 1967. Amorphous/crystalline interrelationships in bone mineral. *Calcif. Tissue Res.* **1**: 8.
9. Termine, J. D., and E. D. Eanes. 1972. Comparative chemistry of amorphous and apatitic calcium phosphate preparations. *Calcif. Tissue Res.* **10**: 171.
10. Termine, J. D., R. E. Wuthier, and A. S. Posner. 1967. Amorphous crystalline mineral changes during endochondral and periosteal bone formation. *Proc. Soc. Exp. Biol. Med.* **125**: 4.
11. Glimcher, M. J., and S. M. Krane. 1968. The organization and structure of bone and the mechanism of calcification. In *Treatise on Collagen*, Vol. 2B. B. S. Gould, editor. Academic Press, Inc., New York. 68.
12. Termine, J. D. 1972. Mineral chemistry and skeletal biology. *Clin. Orthop. Related Res.* **85**: 207.
13. Pellegrino, E. D., and R. M. Blitz. 1965. The composition of human bone in uremia. Observations on the reservoir functions of bone and demonstration of a labile fraction of bone carbonate. *Medicine (Baltimore).* **44**: 397.
14. Kaye, M., A. J. Frueh, and M. Silverman. 1970. A study of vertebral bone powder from patients with chronic renal failure. *J. Clin. Invest.* **49**: 442.
15. Mills, B. G., and L. A. Bavetta. 1968. Bone collagen dynamics. *Clin. Orthop. Related Res.* **57**: 267.
16. Uitto, J., and O. Laitinen. 1968. Relation of collagen metabolism to calcium metabolism in the bone. *Acta Chem. Scand.* **22**: 1039.

17. Avioli, L. V., S. W. Lee, and H. DeLuca. 1971. The metabolism of 25-hydroxycholecalciferol-<sup>3</sup>H (25OHD<sub>3</sub>-<sup>3</sup>H) in uremia. *J. Clin. Invest.* **50**: 4a. (Abstr.)
18. Mechanic, G. L., S. U. Toverud, and W. K. Ramp. 1972. Quantitative changes of bone collagen crosslinks and precursors in vitamin D deficiency. *Biochem. Biophys. Res. Commun.* **47**: 760.
19. Burnell, J. M., and E. J. Teubner. 1973. Acid-base chemistry and human bone. *In* Program, Sixth Annual Contractor's Conference of the Artificial Kidney Program of the National Institute of Arthritis and Metabolic Diseases, Washington, D. C. Feb. 12-14, 1973. 30.
20. Termine, J. D., R. A. Peckauskas, and A. S. Posner. 1970. Calcium phosphate formation in vitro. II. Effects of environment on amorphous-crystalline transformation. *Arch. Biochem. Biophys.* **140**: 318.